Development and progress in resistive plate chamber

CHEN Hong-Fang, WU Jian*

(Department of Modern Physics, University of Science and Technology of China, Hefei 230026)

Abstract Resistive Plate Chamber (RPC) is a robust and low cost gas detector, which is extensively used in high-energy physics, cosmic and astroparticle physics experiments. Over the past twenty years, as a particle detector, RPC has made remarkable progress. The main achievements, features and results of experiemantal tests including R&D and production of the RPCs by several Chinese groups in recent years are reported in this article.

Keywords Resistive Plate Chamber (RPC), Streamer, Avalanche, Multigap Resistive Plate Chamber (MRPC)

CLC number TL811

1 Introduction

Resistive plate chamber (RPC) was developed in 1981.[1] It exploits gas amplification in a uniform electric field between two resistive parallel plates. During the past 20 years, to understand the detector physics and to improve its efficiency, rate capability as well as ageing effect, investigations and developments are lively progressing.[2,3] RPC has several attractive features: large pulse, good time and moderate spatical resolution, mechanical simplicity and robustness. RPC is widely used in high energy physics experiments such as: L3 at CERN,[4] BABAR at SLAC,[5] BELLE at KEK[6] and cosmic ray experiments like GREX/COVER-PLASTEX,[7] EAS-TOP[8] and ARGO[9] experiments at the Yangbajing High-Altitude Cosmic Ray Laboratory, Tibet, China. Future applications will include the muon tracker and trigger detectors for ATLAS, CMS[10,11] ALICE and LHCb experiments at the Large Hadron Collider (LHC), BESIII[12,13] at BEPCII and proposed MONOLITH (Massive Observatory of Neutrino Oscillation or Limits on Their existence) project.

As an important achievement, multi-gap RPC (MRPC) was introduced in 1996[14] in the application of the Time of Flight (TOF) device. MRPC TOF systems are already in use by the HARP[15] experiment at CERN. A prototype of TOF tray[16] has already been run for the ascertainment of a 64 m^2 barrel TOF has been proposed for STAR experiment at RHIC. The 160 m^2 barrel TOF of ALICE[17] will be equipped in the near future.

The study of the RPC's potential as an imaging detector[18] is a very promising start point for possible applications outside particle physics.

Several Chinese groups[11,13,19,20] are working on the R&D and mass production of RPC. With the development of RPCs, we expect that more Chinese laboratories and groups would involve in application and R&D of RPC.

2 Resistive plate chamber (RPC)

The RPC is a DC operated particle detector utilizing a constant and uniform electric field produced by two parallel electrode plates, at least one of which is made of material with high bulk resistivity, such as bakelite and glass, which have a resistivity of $10^{11\pm1}$ $\Omega \cdot$ cm. An example of the configuration is shown in Fig.1. The sensitive element of the chamber is a ~2 mm thick gas layer between the electrodes. The spacers between the electrodes keep the size accuracy of the gap. High voltage is applied to the resistive electrodes. The gas should have high absorption coefficient for ultraviolet light. Normally argon, butane and freon mixture at normal pressure flows through the chamber, which is gas sealed. When the gas is ionized by a charged particle crossing the chamber, the liberated electrons will initiate the electric discharge.

* Corresponding author: wujian@ustc.edu.cn, Tel. +86-551-3601165

Received date: 2004-08-31

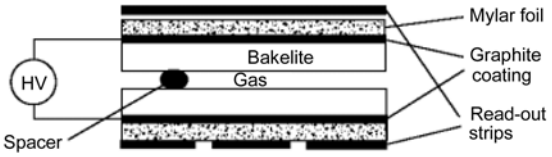

Fig.1 Schematic drawing of the single gap RPC.

The development of a discharge can be summarized into the following steps: (1) Avalanche growth: the average multiplicity of the avalanche that grows past a length l is $\overline{m}(l) = \exp[(\alpha - \eta)l]$, where α is the Townsend coefficient, η is the attachment coefficient.[21] (2) Around a multiplication of 10^5~10^6 the space charge field generated by the avalanche itself starts smoothly to perturb its growth.[22] Due to space charge effects, the effective field acting on the avalanche electrons and therefore the multiplication rate are reduced, it is called saturation phenomenon. As a result, the larger is the avalanche the lower is its growth rate. (3) When the space charge field reaches a critical magnitude, a new discharge propagation mode called streamer, starts rather suddenly.[23] (4) The streamer propagates toward the anode and the cathode, and then a tiny channel of weakly ionized plasma between the electrodes is formed. (5) The spark can develop.[24]

In RPC the discharge is localized and quenched by the following mechanism: (a) prompt switching off the field around the discharge point, due to the large electrode resistivity; (b) UV photon absorption by the butane preventing secondary discharges from gas photo-ionization; (c) capture of electrons of the discharge due to the freon electron affinity, which reduces the size of the discharge and possibly its transversal dimension.

The high voltage is applied to resistive plaste via an electrode with a resistive layer whose surface resistivity is in the range of 10^5~10^7 Ω/square. The resistive electrode is transparent[25] to the transient induced signals, which allows signal pickup copper-pads at ground potential (no high voltage capacitors are used) and makes possible a wide range of design of pickup pad geometries, such as the use of orthogonal strips to achieve a bi-dimensional readout.

Phenolic or melamine-phenolic bakelite is widely used as RPC electrode. The electrode bulk resistivity is an important parameter for the RPC performance. The resistivity of the bakelite changes with temperature and humidity.[26] Another important parameter is the surface smoothness of the plates facing the gas. The bakelite plates of BES III Muon RPC are pressed with dense amine film on the surface to guarantee the smoothness.[13] The average roughness of qualified bakelite is around 0.2 μm.[11] To get high efficiency and low noise rate, some group treated the surface with linseed oil.[27] Float glass with volume resistivity around $10^{11\text{-}13}$ Ω • cm, that has good smooth surface and good planarity, is also used as RPC electrode. But when operating with the freon gas mixture the humidity must be well controlled to assure the performance.[28]

2.1 Streamer mode

RPC was originally operated in streamer mode. In streamer mode, usually the gas mixture used is composed of argon/C_4H_{10}/freon. The electric field in the gas gap is around 4~5.5 kV • mm^{-1}. Very large signals up to ~10^2 pC (1pC = 10^{-12} C) can be achieved, which makes the front-end electronics much simpler to be realized and the experiment operation easier. The streamer mode is used not only for the cosmic ray experiments like ARGO-YBJ but also for the collider experiments like BABAR and BELLE. This operation mode can reach good detection efficiency (~90%) and time resolution (1~2 ns), when a low flux of incident particles is involved. The K_L/μ detector for the Belle experiment is equipped with glass-electrode RPC. Its barrel RPCs are rectangular in shape and vary in size from 2.2 m × 1.5 m to 2.2 m × 2.7 m. The resistivity of glass is as high as ~5×10^{12} Ω • cm, which limits the rate capability of these counter to ~1.0 Hz • cm^{-2}. The signals typically have a 10^2 mV peak into a 50Ω termination and have a full width at half-maximum of less than 50 ns. The efficiency of a single gap is 85%~95%. To provide redundancy and high efficiency (⩾98%), double-gap structure shown in Fig.2 is used. In particular, offsetting the locations of the spacers in the two RPCs could minimize the effects of dead regions near the spacers.

The relaxation time, τ, of discharge for RPC can be estimated from the volume resistivity ρ and the dielectric constant ε of the resistive electrode, as $\tau=\rho\varepsilon$.

The rate capability of RPC depends on how quickly a discharge spot is recharged and therefore depends on the τ. From the optical observation of the streamer images in RPC, the discharge is limited in a 0.4~0.6 cm diameter.[29] So a limited area of 0.2~0.4 cm^2 around the discharge point remains inactive for a dead time of the order of τ. For ρ ~5×10^{12} Ω • cm and ε ~$7\varepsilon_0$ of glass, then τ is ~3 s, which limits the rate capability. It should be noticed that this is just a naive estimation, and both charge spread and conduction on the surface are not included.

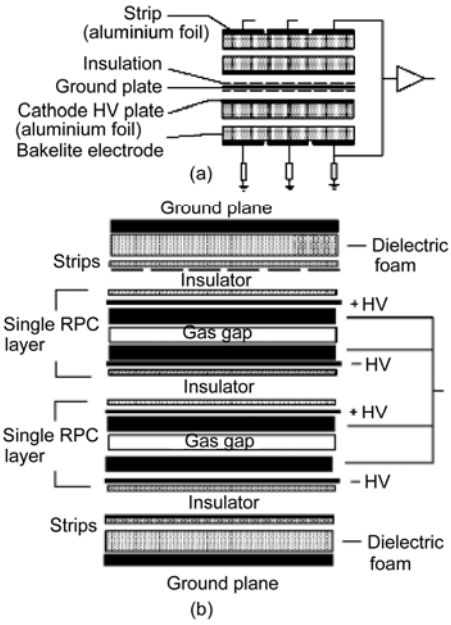

Fig.2 Two kinds of double gap RPC configuration
(a) High Voltage (HV) inverted double gap, (b) HV parallel double gap.

2.2 Avalanche mode

In recent years, the applications of RPC at LHC experiment require high rate capability ~10^3Hz • cm^{-2}. RPCs at high flux begin to lose their efficiency, due to the fact that, after the streamer development, the area of electrode plates involved in the discharge needs a certain time to get recharge. A way to solve this problem is to use the plates of lower resistivity (~10^{10} Ω • cm) and operate RPC in the low gas gain mode, which is usually referred as avalanche mode, to reduce the size and charge of the avalanche and the corresponding electrode discharge area. For this reason, the discharge development should be controlled to stop before the formation of streamer. RPCs operated in avalanche mode have been proposed as the dedicated detector both in CMS and ATLAS at LHC. The basic problem is to operate the RPC in avalanche mode with high efficiency, wide HV plateau and a very low contamination of streamers. The performance of the RPCs in low gas amplification mode has been studied in term of rate capability, electric discharge inside the RPC, its evolution with increasing electric field and the effect of gas mixtures. The avalanche amplitude was observed to be exponentially dependent on the operating voltage to a value, characteristic of the gas, where saturation occurs and delayed streamer signals start to appear. For a RPC with 2 mm gap and 2 mm bakelite electrode, the waveform observed refers to a gas mixture of argon/n-C_4H_{10}/$C_2H_2F_4$ in the ratio of 10/7/83 in volume as shown in Fig.3, where multiple streamer signals are frequently visible with the voltage above 11 kV.[30]

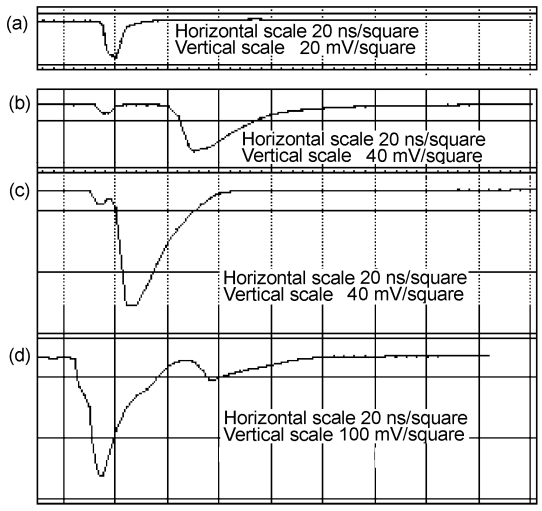

Fig.3 The signal waveform at different operating voltage
(a) An avalanche signal (at 9.4kV) has a typical duration 4~5 ns FWHM; (b) A streamer signal follows the avalanche with a delay of 38 ns at 9.6kV; (c) The avalanche to streamer delay becomes shorter at 10.2kV; (d) The avalanche and streamer signals merge into a single pulse at 11.4kV. Multi-streamer signals are also observed.

For most gases, a high fraction of freon is preferred; this gas exhibits attractive features like electron affinity and a high primary ionization (~10 cluster • mm^{-1}). The $C_2H_2F_4$ (R134a) is preferred, because it is an ecologically acceptable freon for its negligible world warm effect. The voltage range in which RPC can be operated in avalanche mode is limited by the appearance of the streamer. For RPCs to operate in avalanche mode and with longer voltage range, groups

have been working to search the streamer suppressing gases.

The addition of small amounts of sulphur hexafluoride (SF_6) to the mixture $C_2H_2F_4$/ C_4H_{10}, 97/3, has the effect of suppressing the streamer in a very large interval of operating voltages. The absence of streamers makes the avalanche working in the saturation region, thus attractive for RPC though SF_6 will make RPC operating at higher voltage. Fig.4 shows the detection efficiency and streamer probability versus operating voltage, where there is a >1 kV operation voltage plateau in pure avalanche mode with detection efficiency >98%, if only 1% SF_6 added.[31]

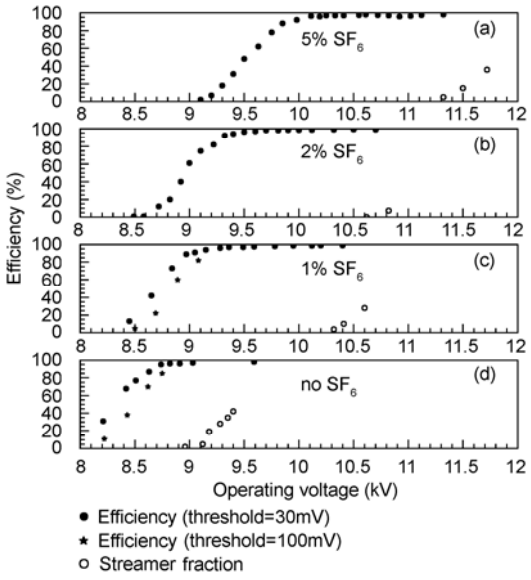

Fig.4 Detection efficiency and streamer probability vs. operating voltage for
(a)5%, (b) 2%, (c) 1% SF_6 concentration and (d) no SF_6.

Operated in avalanche mode, the rate capability of a RPC is determined by the volume resistivity ρ of the electrode and scales roughly as $1/\rho$. For this reason, RPCs used in experiments working at high rates are generally built with bakelite electrode, that can be produced with resistivity as low as 10^9 Ω • cm. Fig.5 shows the efficiency could be higher than 90% at rate of kHz • cm^{-2}. A consistent improvement in the rate capability has been achieved.[32,33]

According to the experience, the RPC operating electric field decreases with the gap size at a lower rate. The simplest functional relationship between the voltage V and the gap size g, for fixed pressure and temperature, is of type

$$V = Kg^{\gamma}$$

where K and γ are the parameters depending on the gas and operating mode, $0<\gamma<1$. K and γ can be obtained by fitting the existing data on different gases for both avalanche and streamer mode operation.

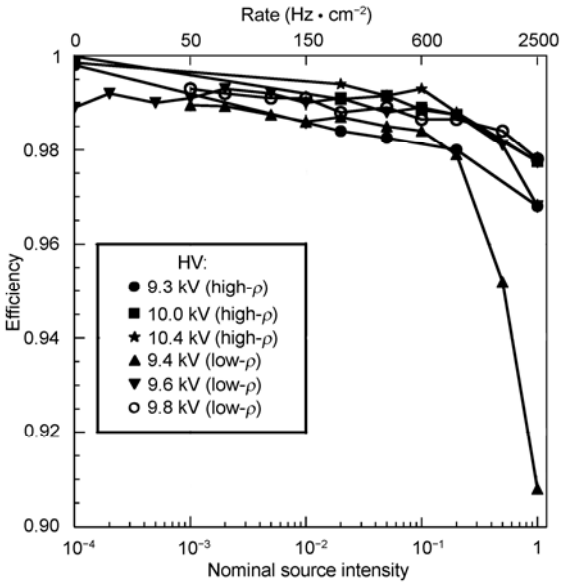

Fig.5 The efficiency of a 2 mm gap RPC as a function of the flux rate at different HV values for different bakelite bulk resistivity (low ρ: 5×10^8 Ω • cm, high ρ: 3×10^{10} Ω • cm).

For small changes of pressure and temperature, based on a linear scaling of the voltage with the gas density, the operating voltage is usually corrected by scaling the applied voltage V_a according to the relationship

$$V = V_a \frac{P_0 T}{P T_0}$$

where P and T are the operating pressure and temperature, V is the effective operating voltage scaled at some standard pressure P_0 and temperature T_0. The effect of a large change of pressure should be equivalent to a proportional change in gap size and therefore the corresponding scaling of the voltage is not linear.[34]

The aging effect is also very important for the application of RPCs. Various tests have been made. The aging studies concerned most of the materials of the RPC components: bakelite or glass resistive plate, graphite electrodes (or surface painting), surface coating (like linseed oil coating) and the chemical etching of the electrode inner surface by fluorine ions (the fluorine compounds delivered by the discharge). In avalanche mode operating under gamma irradiation with count rate ~10^2 Hz, and a total discharge charge

above 0.05 C • cm^{-2} in gap accumulated, the performance of RPC shows no aging effect.[35,36]

2.3 Multigap resistive plate chamber (MRPC)

The first multigap resistive plate chamber (MRPC) is proposed in 1995. The original goal is to improve the time resolution of the wide gap (8 mm) RPC to be as good as the 2 mm gap RPC, and keep the advantages of the wide gap (8 mm) RPC: higher rate capability and lower power dissipation.[37] Further R&D work on application of the MRPC for Time of Flight (TOF) detectors showed that it can reach a time resolution better than 70 ps and be proposed for the very large area TOF array of the heavy ion collision experiment-ALICE at the CERN LHC.[38-40]

The MRPC consists of a stack of resistive plates. Spacers between these plates define a series of gas gaps. An anode and cathode electrodes are connected to the outer surfaces of the outermost resistive plates. All internal plastes are electrically floating. The basic features of MRPC are: (a) the internal plates take the correct voltage initially by the electrostatics and are kept at the correct voltage due to the flow of electrons and positive ions created in the avalanche process. (b) the resistive plates are transparent to the fast signals generated by the avalanches indside each gas gap. The induced signal on the external electrodes is the sum of the charges of all the gaps. Fig.6 shows the cross section of a single stack MRPC with 6 gas gaps.

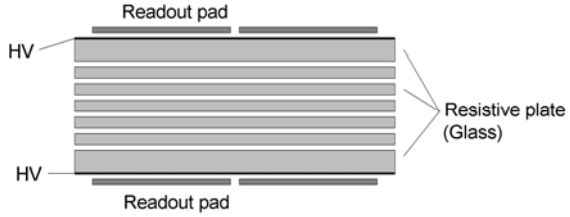

Fig.6 Gross section of a single stack MRPC with 6 gas gaps

For timing detector, the important character is the time resolution. In parallel plate chamber, the signal is generated by avalanche across the gap. The number of electrons, N, in an avalanche is given by $N=N_0e^{\alpha^* l}$, where α^* is the effective Townsend coefficient ($\alpha^*=\alpha-\eta$); l is the distance of avalanche that has been progressed from its initial position; and N_0 is the initial number of electrons in the primary ionization clusters. Thus the generated signal depends on the position of primary ionization clusters. Applying a threshold to the signal gives a threshold cross time. The variation of the position of the primary cluster and the avalanche fluctuation generate the time jitter. The time resolution could be given by $\sigma_t \propto 1/(\alpha^* v_d)$, where v_d is the drift velocity of electron in the gas. From the program to compute energy loss of fast particle in gas HEED (I. Smirnov) and gas transport IMONTE, MAGBOLTZ (S. Biagi), for gas mixture $C_2H_2F_4$/i-C_4H_{10}/SF_6 at normal pressure, 9~10 primary clusters/mm will be produced by ionization of fast charged particles. The Townsend coefficient and drift velocity related to electric field predicted by these program are shown in Fig.7. With the electric field ~10 kV • mm^{-1}, the effective Townsend coefficient is about 100 mm^{-1}, the dirft velocity is ~200 μm • ns^{-1},[41] $1/(\alpha^* v_d)$ reaches ~50 ps (1 ps=10^{-12}s).

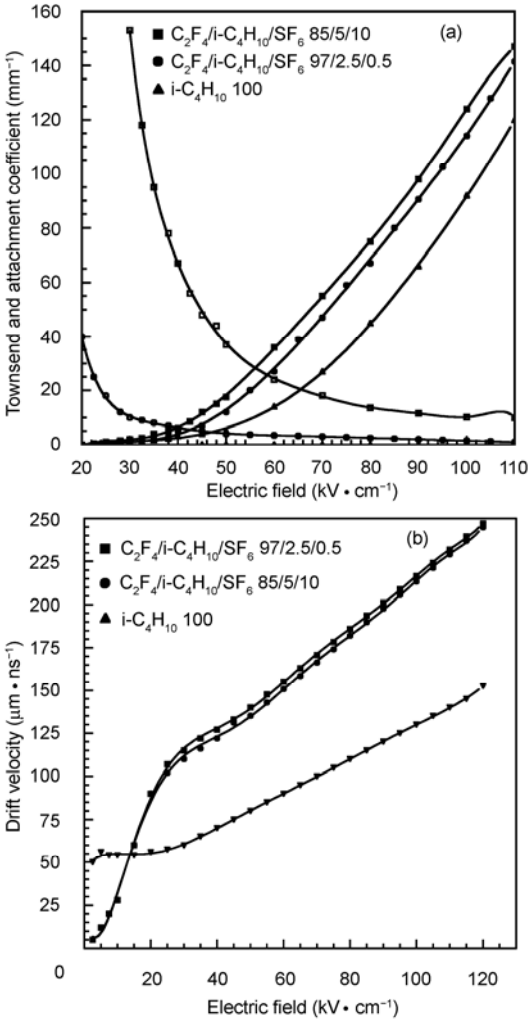

Fig.7 (a) Townsend (solid symbol) and attachment (open symbol) coefficient simulated with IMONTE. (b) Drift velocity simulated with MAGBOLTZ.

RPC with gas gaps as thin as 0.2~0.3 mm could work at avalanche mode with high value of α^* and v_d. The lower efficiency, due to the thin gas gap, can be compensated by increasing the number of gaps as in the multigap version. For Multigap RPC the resistive plates are float glass, the thickness of internal glass plates in the range of 400 μm ~ 1.1 mm and the external glass plates in the range 550 μm ~ 2 mm have been used. Nylon fishing line (its diameter error is in the range of 2~3 μm) is used as spacer between the glass plates. The voltage is applied to the exterior glass surface using graphite tape (or resistive painting) with a surface of 10^5~10^6 Ω/square. A layer of Mylar of 350 μm thick is used to insulate the HV from the readout pads. Each pad is connected to a fast amplifier. The output of the amplifier is split into two, one to the discriminator and then fed to a Time Digital Converter (TDC), and the other one further amplified and fed to the Analog Digital Converter (ADC). The time over discriminator's threshold of the pulse leading edge and the total charge of the signal are then measured. The electric field in the gas is around 10~12 kV • mm^{-1}, operating in the $C_2H_2F_4$/iso-C_4H_{10}/SF_6 gas mixture. For a 1.2 m×7 cm strip with 96 readout pads (the area of each pad is 2.5 cm×3.5 cm), the beam test results for different gap sizes are shown in Fig.8. A time resolution around 70 ps is achieved.[39]

To obtain longer efficiency plateau and operate at lower high voltage, double stack of MRPC was built, one example of the structure is shown in Fig.9.[42] Testing with a collimated 7 GeV/c pion beam, efficiency and time resolution of this MRPC is shown in Fig.10. The character of 10 gap MRPC is much improved, around 50 ps of time resolution and >98% of efficiency are reached.

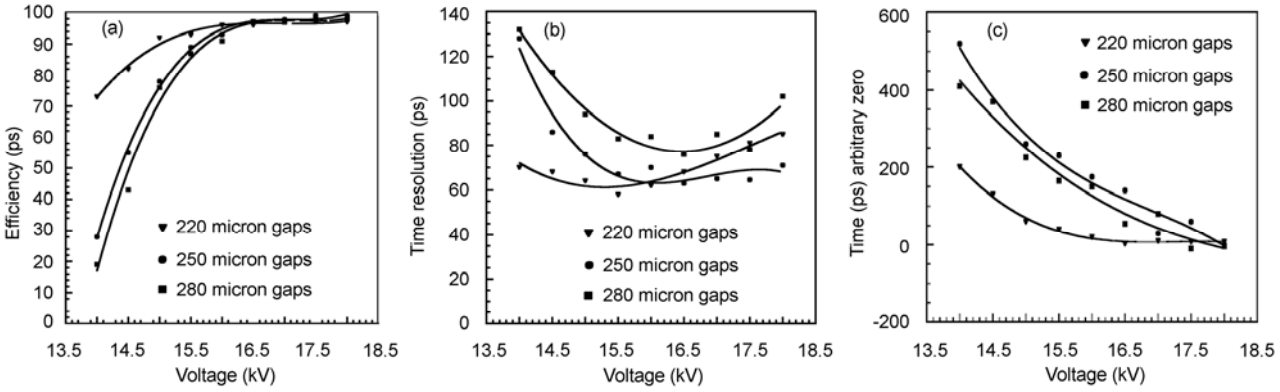

Fig.8 Efficiency, time resolution and time walk as a function of high voltage.

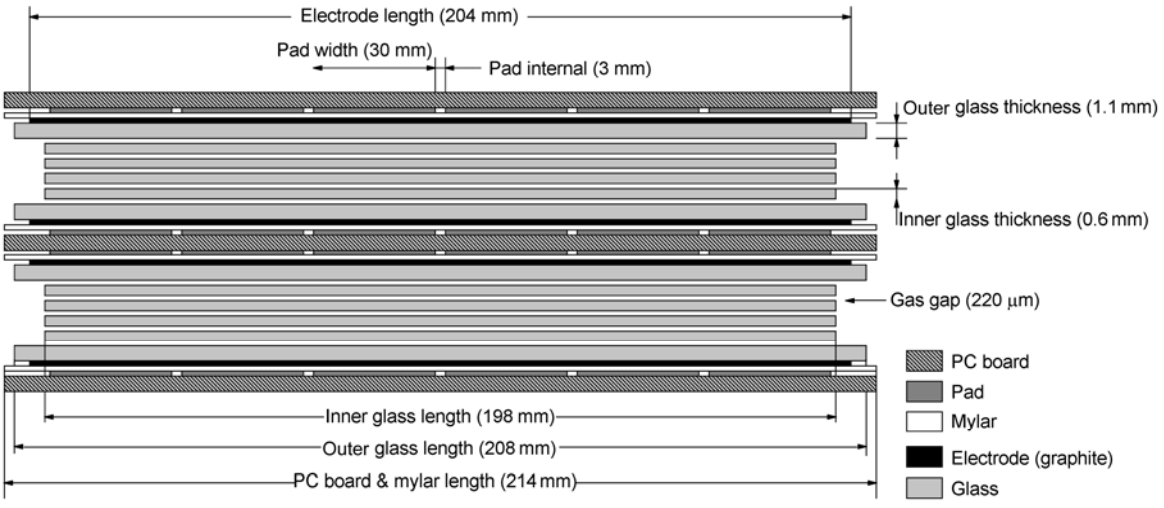

Fig.9 A double stack of 5-gap MRPC.

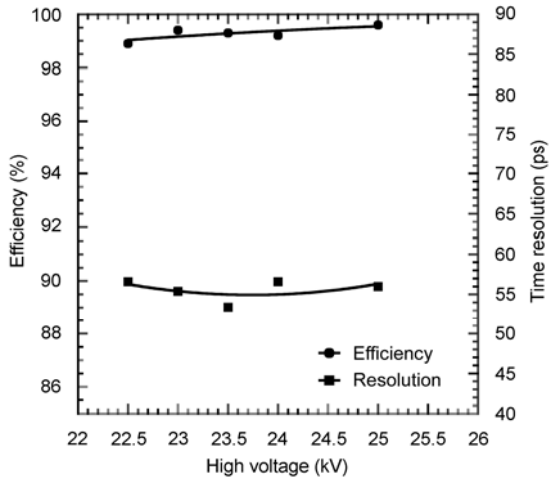

Fig.10 Efficiency and time resolution of a 10 gap MRPC.

The rate capability of a double stack MRPC with 10 gaps (each stack has five 250 μm gaps) of ALICE group was tested at the Gamma Irradiation Facility (GIF) at CERN. Fig.11 shows the efficiency and time resolution as a function of the rate of charged particle.[39] In the flux, due to the current drawn by MRPC the voltage across the glass stack drops, so the real effective voltage on the MRPC is lower than the nominal applied voltage. In Fig.11 the effective voltage is the effective voltage on MRPC.

Each pad of MRPC is read out individually. On the PC board, between the pads there are distances of 2~3 mm, so 'charge sharing' effect is present between adjacent pads. The increased number of gaps (from 6 to 10) results in collecting larger signal. The other important factor is that the size of the induced charge distribution of avalanche on the readout pads will be larger than the 6 gaps. A resistive layer on the electrode also adds a spreading effect. Fig.12 shows the time resolution distribution with the beam position along the pads. From the figure we learn that using higher resistivity, the time resolution along the pad is more uniform.

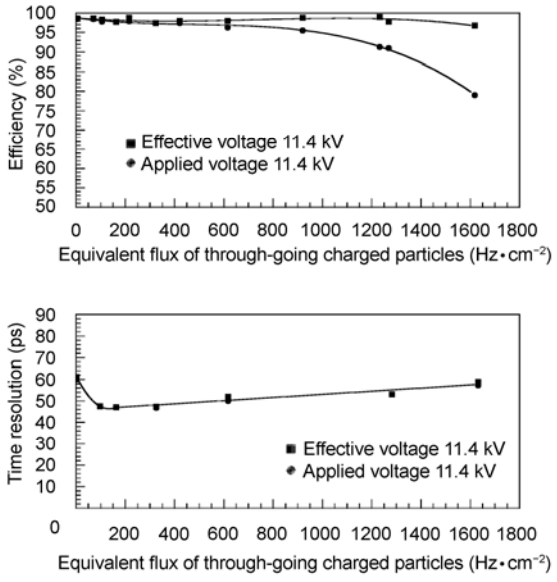

Fig.11 Efficiency and time resolution as a function of the rate of charged particles.

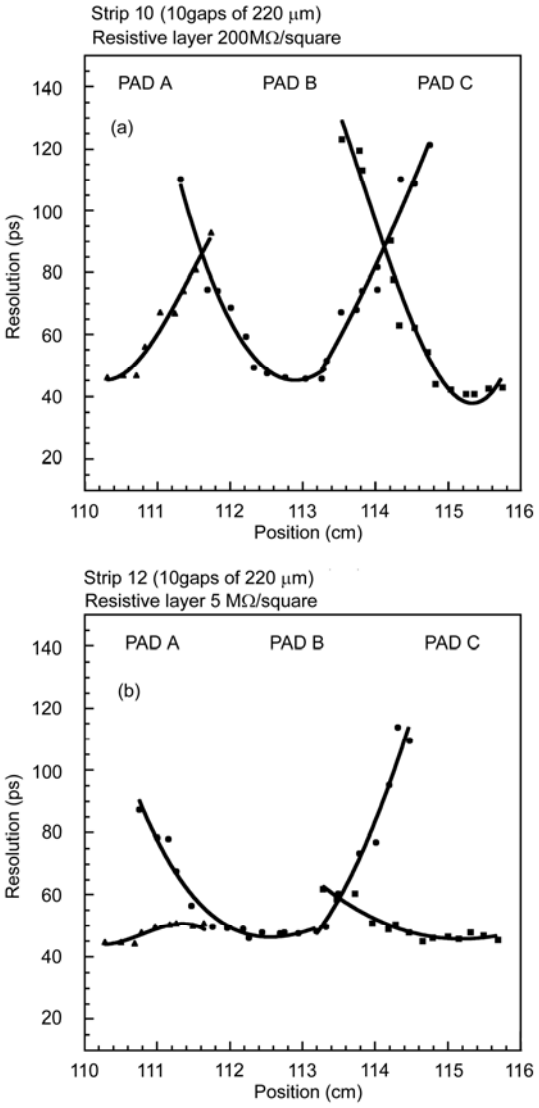

Fig.12 Time resolution distribution along the pads for 200kΩ/square (a) and 5MΩ/square (b) resistive layers on the electrodes.[40]

MRPC as a TOF detector has many attractive features: high detection efficiency (>95%), excellent intrinsic time resolution (<100 ps), good rate capability (10^2~10^3 Hz • cm^{-2}), large acceptance, ability to operate inside the magnetic field and low cost. For the

experiment of heavy ion collision, the high particle multiplicity of final state dictates demanding requirement of high granularity of detector. Using the traditional methodology based on scintillators and photo-multipliers can hardly meet the entire mentioned requirement. But MRPC is such a detector, which could fit these requirements. The TOF system (10 m^2, 368 readout channels) of HARP experiment was already operating, which consisted of double stack of two gaps of 0.3 mm MRPC. A time resolution of ~150 ps and an efficiency of ~99% were obtained. A prototype of STAR barrel TOF system consisting of twenty eight single stack 'six gaps of 0.22 mm' MRPCs has been operated in the experiment in RHIC (BNL), an average time resolution of ~85 ps and an efficiency of ~95% are reached. The proposed TOF detector of ALICE experiment will have an active area of ~160 m^2 and ~160,000 readout channels.

3 Conclusion

RPC working at both avalanche and streamer mode could obtain a time resolution of ~1 ns and an efficiency of ~90%. Efficiency above 99% is reached by use of two or more gaps. The counting rates of ~10^2 Hz • cm^{-2} in avalanche mode and ~10 Hz • cm^{-2} in streamer mode are routinely achieved.

An important achievement in the RPC application is the progress in the timing capability. Many experimental data showed that thin gas gaps (0.2~0.3 mm) RPCs can achieve a time resolution of ~50 ps, definitely better than 100 ps.

RPCs have already been widely accepted in high energy experimental physics and astroparticle field, for its robustness, good time resolution and relative low cost.

RPCs with special configurations such as second electron emitters and micro-strip readout[43] and micro-gap RPCs,[44] are being developed. To study the potential of RPC as an imaging detector, RPC-PET,[17] is a very promising starting point for possible application in other fields. Future task for developing RPCs would be improving the detector physics understanding, management and control of an unprecedented large mass production (10^4 m^2), and developing new configuration for the application in other fields.

References

1 Santonico R, Cardarelli R. Nucl Instr Meth, 1981, **187**: 377-380

2 Cardarelli R, Santonico R. Nucl Instr Meth, 1988, **A263**: 20-25

3 Fonte F. IEEE NS, 2002, **49**(3): 881-887

4 Aloisio A, Alviggi M G, Patricelli S *et al*. Nucl Instr Meth, 2000, **A456**: 113-116

5 Zallo A. Nucl Instr Meth, 2000, **A456**: 117-120

6 Yamaga M, Abashian A, Abe K *et al*. Nucl Instr Meth, 2000, **A456**: 109-112

7 Ambrosio M, Aramo C, Colesanti L *et al*. Nucl Instr Meth, 1996, **A381**: 64-72

8 Ambrosio M, Aramo C, Battistoni G *et al*. Nucl Phys B (Proc Suppl), 1999, **75A**: 315-317

9 Bacci C, Bao K Z, Barone F *et al*. Nucl Instr Meth, 2003, **A508**: 110-115

10 CMS Muon Project, Technical Design Report, 1997

11 Ying J, Ye Y L, Ban Y *et al*. J Phys, 2000, **G26**: 1291-1298

12 BESIII Design Report

13 ZHANG Jiawen, ZHAO Haiquan, LI Rubai *et al*. High Energy Physics and Nuclear Physics (in Chinese), 2003, **27**: 615-618

14 Zeballos E, Crotty I, Hatzifotiadou D *et al*. Nucl Instr Meth, 1996, **A374**: 132-135

15 Bogomilov M, Dedovich D, Dumps R *et al*. Nucl Instr Meth, 2003, **A508**: 152-158

16 Bonner B, Chen H, Geary G *et al.* Nucl Instr Meth, 2003, **A508**: 181-184

17 Williams M C S. Nucl Instr Meth, 2002, **A478**: 183-186

18 Blanco A, Carolino N, Marques R F *et al*. RPC 2003 VII workshop on RPCs

19 SHAO Ming, CHEN Hongfang, LI Cheng *et al*. High Energy Physics and Nuclear Physics (in Chinese), 2004, **28**: 733-737

20 LI Cheng, WU Jian, WANG Xiaolian, *et al*. Nuclear Science and Techniques, 2002, **13**:6-10

21 Riegler W, Lippmann C. Nucl Instr Meth, 2003, **A508**: 14-18

22 Abbrescia M, Colaleo A, Iaselli G *et al*. Nucl Phys B (Proc Suppl), 1999, **78**: 459-464

23 Duerdoth I, Clowes S, Frestone *et al*. Nucl Instr Meth, 1994, **A348**: 303-306

24 Kitayama I, Sakai H, Teramoto Y *et al*. Nucl Instr Meth, 1999, **A424**: 474-482

25 Battistoni G, Campana P, Chiarella V *et al*. Nucl Instr Meth, 1982, **202**: 459-464
26 Arnaldi R, Baldit A, Barret V *et al.* Nucl Instr Meth, 2000, **A456**: 140-142
27 Anulli F, Bagnasco S, Baldini R *et al*. Nucl Instr Meth, 2000, **A508**: 128-132
28 Abashian A, Abe, K Abe, *et al*. Nucl Instr Meth, 2000, **A449**: 112-124
29 Abe K, Hoshi Y, Kumagai K *et al*. Nucl Instr Meth, 2003, **A508**: 34-37
30 Cardarelit R, Makeev V, Santonico R. Nucl Instr Meth, 1996, **A382**: 470-474
31 Camarri P, Cardarelli R, Di Ciaccio A *et al*. Nucl Instr Meth, 1998, **A414**: 317
32 Cwiok M, Dominik W, Gorski M *et al*. Nucl Instr Meth, 2000, **A456**: 87-90
33 Adinolfi M, Carboni G, Messi R *et al*. Nucl Instr Meth, 2000, **A456**: 95
34 Santonico R. Nucl Instr Meth, 2000, **A456**: 1-5
35 Abbrescia M, Colaleo A, Guarrasi L *et al*. Nucl Instr Meth, 2002, **A477**:293
36 Carboni G, Collazuol G, De Capua S *et al*. Nuclear Physics B (Proc Suppl), 2003, **125**:374-379
37 Zeballos E C, Crotty I, Hatzifotiadou D *et al*. Nucl Instr Meth, 1996, **A374**: 132-135
38 Akindinov A, Anselmo F, Basile M *et al*. Nucl Instr Meth, 2000, **A456**: 16-22
39 Williams M C S, Nucl Instr Meth, 2002, **A478**: 183-186
40 Antonioli P. Nuclear Physics B (Proc Suppl), 2003, **125**: 193-197
41 Riefler W, Lippmann C. Nucl Instr Meth, 2003, **A508**: 14-28
42 Shao M, Ruan L J, Chen H F *et al*. Nucl Instr Meth, 2002, **A492**: 344-350
43 Zeballos E, Crotty I, Hatzifotiadou D *et al*. Nucl Instr Meth, 1997, **A392**: 150-154
44 Fonte P, Peskov V. Nucl Instr Meth, 2000, **A454**: 260-266